Bias Tees Integrated Liquid Crystals Inverted Microstrip Phase Shifter for Phased Array Feeds

Jinfeng Li
Department of Electrical and Electronic Engineering
Imperial College London
London SW7 2AZ, United Kingdom
jinfeng.li@imperial.ac.uk

***Abstract*—Microwave phase shifters based on tunable dielectrics such as nematic liquid crystals (NLC) have attracted considerable research attention in the last two decades. To electronically drive the permittivity variations based on the NLC's molecular anisotropy, conventional device configuration is based on externally wiring three-port bias tees as diplexers for frequency-domain multiplexing, i.e. isolating the RF port from the low-frequency high-amplitude bias field. The multi-stage bulky solution significantly impedes its applicability for phased array feeds. To the best of the author's knowledge, limited research has attempted the integration of compact bias tees into the phase shifter. To this end, this work demonstrates a bias-tees-embedded standalone phase shifter integrated on a double-sided RO4003 substrate using advanced fabrication and assembly techniques (photolithography, surface mounting, reflow soldering). The measured differential phase shift reports 391.75° at 10 GHz with the insertion loss up to -5.66 dB (including bias tees) for an optimised design. A figure-of-merit of 69°/dB is achieved, which even outperforms recent advances in NLC-based planar phase shifters without bias tees.**

Keywords—bias tee, liquid crystal, microwave integrated circuit, phased array feeds, phase shifter, vias optimisation

I. Introduction

Historically, microwave phased array antennas [1] are fed by variable phase shifters realised in semiconductor switches [2], micro-electro-mechanical systems (MEMS) switches [3], ferrites [4], or ferroelectrics [5] delay lines. These technologies exhibit sufficiently fast switching response in microseconds, but suffer two major drawbacks, i.e. the binary resolution in phase shifting (owing to the digital switching nature), and the large insertion loss (due to the intrinsic absorption in materials), both of which impede the commercialisation of phased arrays for consumer electronics. In the recent two decades, nematic liquid crystals (NLC) [6]–[10] have shifted the limits of the phase-shifting resolution and amplitude attenuation by providing continuous (analog) phase tuning and ultra-low dissipation factors that are out of reach by the classical solid-state or ferroelectric materials. In particular, meandering microstrip-line architecture has been attempted extensively [11] for NLC-based planar circuit implementations. However, most of these studies have yet to consider incorporating the biasing networks systematically into the optimisation scope, to be more specific, the bias tee component that multiplexes the microwave signal (to be transmitted) and the low-frequency bias voltage (to control the NLC dielectric constant for phase tuning). Fig. 1 illustrates the traditional bulky three-port externally connected bias tees, as compared with a compact surface-mount bias tee (TCBT-14+ from Mini-circuits) proposed for use in this work. Arguably, the overall setup size reduction at a very low cost is a fundamental challenge that remains to be solved for NLC-based large-scale phased array feeds, comprising hundreds, if not thousands of radiating elements.

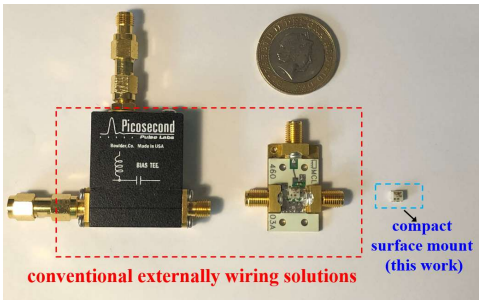

Fig. 1. Size comparison of traditional externally wired bias tee solutions (left), and novel surface-mount integrated solution (right) in this work.

To this end, this paper works on the surface-mount bias tees embedded solution towards the systematic integration of the NLC phase shifters with transmitters or receivers. Section II studies the impact of microwave transmission line geometry on the phase tuning range, with a special focus on the NLC-tailored mixed-signal circuits design and the optimisation of copper-filled vias. Section III presents the assembled standalone phase shifter prototype and the measurement results for comparison with the state-of-the-arts.

II. NLC Standalone Phase Shifter Device Design

A. Effect of Device Configurations on Phase Tuning Range

The earliest transmission method by twin lines no longer works for microwave frequencies because of the open-nature and high radiation losses. This accounts for the employment of classical coaxial cables designed in a closed structure, which has subsequently evolved into planar transmission-line structures such as a strip line sandwiched between two conductor plates, and a microstrip line printed on top of a dielectric substrate.

For a NLC-filled coaxial transmission line, a core conductor is embedded in the lossy NLC tunable dielectrics, exhibiting a non-planar transverse electromagnetic (TEM) mode with a radially polarised electric field. This structure features high isolation and radiation-free properties up to the cut-off frequency, beyond which the higher-order transverse electric mode TE_{11} comes into play. From the wave-occupied volume ratio ($WoVR$) point of view for the coaxial structure with NLC surrounding a core line, 100% of the microwave signal is confined in the tunable dielectrics without leakages, thus the device tuning range (TR) can theoretically reach the NLC's material tunability. In this regard, it seems that the theoretically highest tuning range can be realised in this structure. However, it is not the case due to the impossibility of achieving the extreme value of the permittivity $\varepsilon_{r,\perp}$ for the bulk dielectric volume. By ways of illustration in the cross section shown in Fig. 2, it depicts the mixed signals coexistence for NLC biasing (using low-frequency voltage),

and microwave signal transmission. Due to its radial and non-planar nature, it is technically infeasible to create a radial surface-anchoring effect by mechanically rubbing an alignment film (Fig. 3) onto the tiny core (diameter in the order of 0.2 mm at 10 GHz), because maintaining the core's structural integrity is challenged. Instead, a magnetic field (the right of Fig. 2) can be used for NLC alignment, but this results in high power consumptions and a large footprint due to the request for permanent magnets. The impossibility of switching from $\varepsilon_{r,\perp}$ leads to a degradation of the tunability and hence the tuning range of the structure, which cancels out the advantage of the 100% wave-occupied-volume ratio (*WoVR*). Furthermore, from the insertion loss point of view, the metal ohmic loss is obtained by integrating the square of the microwave field intensity over the effective surface areas of the entire core and the entire metallic shield (ground). The substantial effective surface areas of this structure to be integrated account for a large metal loss compared with that using planar transmission-line solutions. Due to a combination of the lossy problems, no ease of alignment, lack of mechanical stability, and technically demanding for integration, such a coaxial structure is suitable only for NLC material characterisation purpose at the lower frequency range of microwave. Strip line, a semi-planar structure suffers from identical disadvantages as with coaxial when combining with NLC for device considerations. In conclusion, NLC-based phase shifters realised in a coaxial or strip line structure struggle to meet the quest for low-loss, low-power consumptions and compactness. For the wavelength range below 30 GHz, inverted microstrip is the optimal topology with planar advantages for integration with the relatively mature NLC technology. The inverted microstrip employed in this work is a 0.5 oz copper core line patterned on a RO4003 substrate, and a Duralumin substrate as ground plane, separated by NLC as tunable dielectrics.

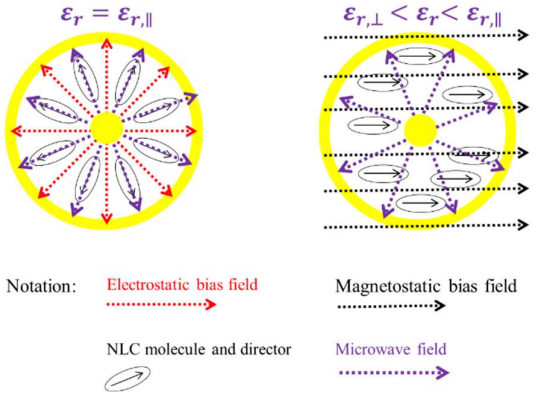

Fig. 2. NLC coaxial phase shifter biased by electric or magnetic fields.

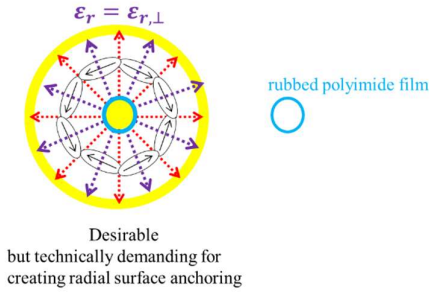

Fig. 3. Imaginary depiction of NLC anchored by radial surface alignment.

B. *Packaging Design with Bias Tees Integration*

High Frequency Structure Simulator (HFSS from Ansys) is used to design the standalone phase shifter comprising the NLC-filled inverted microstrip delay line integrated with bias tees. A pair of TCBT-14+ bias tees and impedance-tuning capacitors (0.01 μF) are surface-mounted on the top side of the RO4003 substrate. The use of the miniaturised TCBT-14+ is spurred by the compact size and wideband capability from 10 MHz to 10 GHz. Fig. 4 is a perspective view of the whole device decomposed into layers. The optimised dimensions for the meandered microstrip and the biasing network are schematically shown in Fig. 5 (a) and (b), respectively.

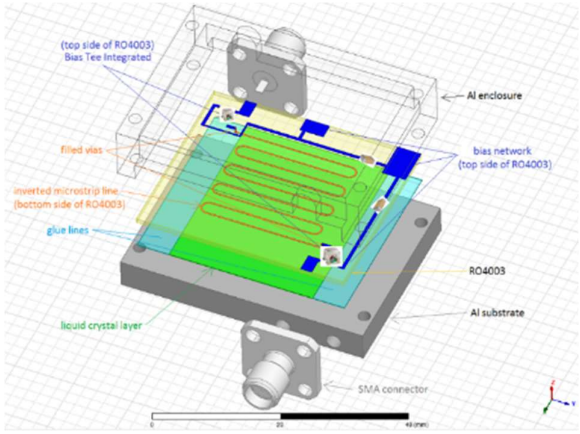

Fig. 4. Perspective view of the proposed standalone solution of the bias tees integrated liquid crystal microwave phase shifter.

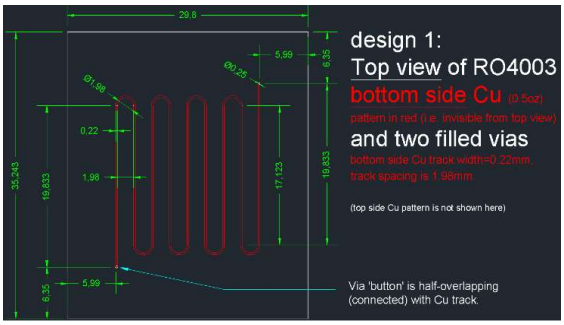

(a)

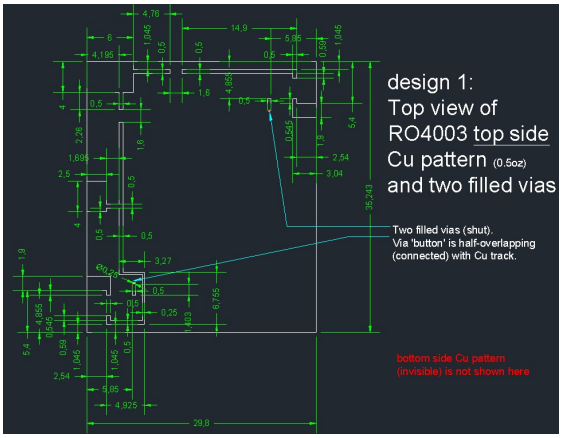

(b)

Fig. 5. Design dimensions of (a) microwave inverted microstrip (RO4003 bottom side); (b) low-frequency biasing network (RO4003 top side).

C. Vias Optimisation

The nature of electrically isolating the low-frequency biasing network and the microwave-frequency signal line requires a double-sided circuit as implemented in Fig. 6, i.e. top launch microstrip line with plated-through-hole vias interconnecting the meandering microstrip on the bottom side. It is worth noting that the vias as a type of discontinuity in the signal line exhibit a lower impedance as compared with that of the planar transmission line on PCB. The resulting higher-order modes' radiation and reflection increase the insertion loss. By simulation, the increase in the insertion loss mainly depends on the ratios of the height of the vias to the guided wavelength (λ), i.e. vias height should be below one-tenth of the guided λ to mitigate resonance, undesirable couplings, and radiations. At 10 GHz, the guided λ is 18.96 mm for the inverted microstrip architecture, thus the limit of the via height (substrate thickness) is up to 1.8 mm.

Furthermore, conductor-filled vias exhibit additional inductance and hence a lower mismatching loss as compared with non-conductive resin-filled plugged vias and tenting vias that are closed with solder mask. To minimise the losses whilst targeting mechanical stability for the sake of the NLC layer's uniformness, vias are plated shut with copper (0.25mm in diameter), and the commercially available RO4003 substrate with a thickness (representing the vias' height) of 0.813 mm is employed. The associated pad size can also enhance the inductive effect to reduce the impedance mismatching, as investigated by the button pad case (pad diameter = 0.4 mm) shown in Fig. 7 (a), as compared with the no button pad case (pad diameter = 0.25 mm) shown in Fig. 7 (b). As evidenced by the simulation results reported in Fig. 8, the button pad mitigates the return loss S_{11} (especially for 1-6 GHz under 0 V bias), and slightly improves the forward transmission S_{21}.

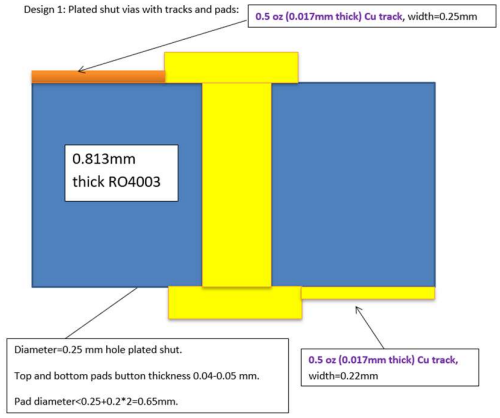

Fig. 6. Optimisation of copper-filled vias to minimise geometrical discontinuity-induced high-order modes at 10 GHz.

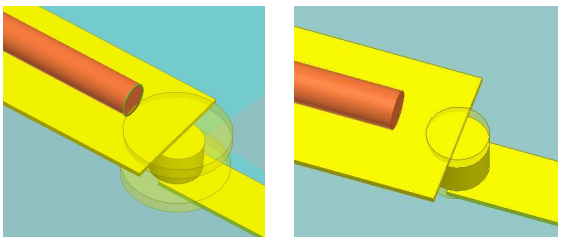

(a) (b)

Fig. 7. Effect of pad diameter (a) 0.4 mm; (b) 0.25 mm on insertion loss.

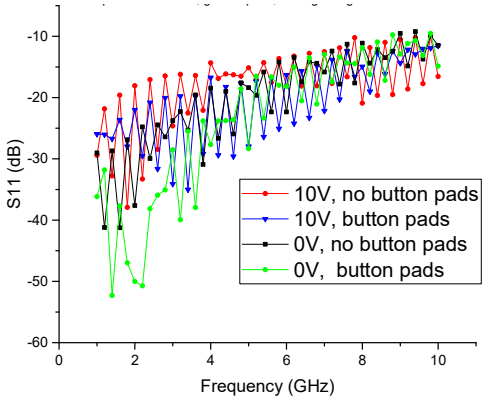

(a)

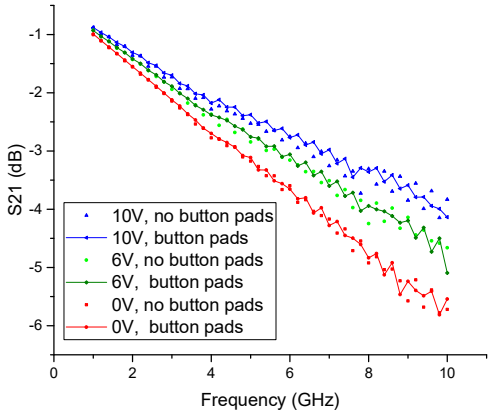

(b)

Fig. 8. Simulated (a) return loss; (b) insertion loss of the bias tees embedded NLC phase shifter (copper-filled vias with and without button pads).

III. Measurement of Device Performance

The microstrip line is fabricated by photolithography and chemical etching, with the NLC filled and encapsulated based on established LC-based device assembly techniques [6, 7, 12]. Surface mounting of the bias tees and capacitors is performed by reflow soldering through a reflow oven (CIF - F31114). An aluminum alloy enclosure is mounted by screws, targeting radiation confinement and crosstalk shielding. The assembled device is presented in Fig. 9 with a size illustration.

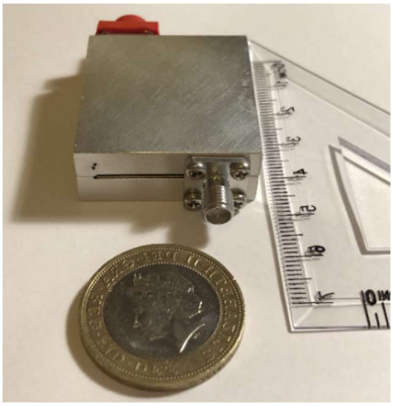

Fig. 9. Image of the fabricated NLC standalone phase shifter with embedded bias tees (inside the enclosure) and assembled SMA connectors.

The fabricated NLC standalone phase shifter device prototype is experimentally characterised using a two-port vector network analyser directly connected to the SMAs of the device without introducing junctions and external bias tee components. Measurement results of the S parameters are presented in Fig. 10, reporting a phase-shifting capability of 391.75° at 10 GHz (18 V bias, with enclosure), and an insertion loss from a minimum of -4.04 dB (18 V, with enclosure) to a maximum of -5.66 dB (0 V, with enclosure), i.e. a figure-of-merit (defined by the maximum phase shift to the maximum insertion loss) of 69°/dB is achieved, an improvement of 10% as compared with the state-of-the-art [13] liquid crystal inverted microstrip based phase shifter at 10 GHz.

While the measured differential phase shift performance is not sensitive to the enclosure according to Fig. 10 (a), the metal housing effectively screens out the radiation and crosstalk losses and thus improves the forward transmission S_{21} by up to 0.48 dB at 10 GHz, as evidenced in Fig. 10 (b). Arguably, there is a huge opportunity for optimisations both numerically [14]–[25] and experimentally [26]–[29] based on the ongoing investigations into the materials' absorption losses in metals and dielectrics.

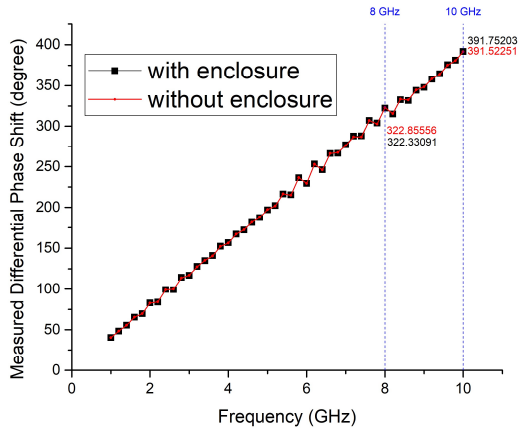

(a)

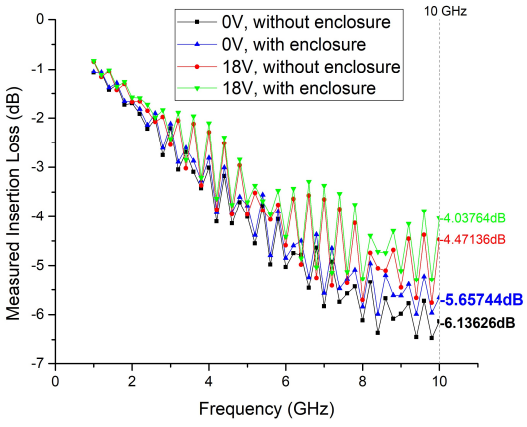

(b)

Fig. 10. Measured (a) differential phase shift; (b) insertion loss of the prototyped NLC phase shifter device with bias tees embedded.

IV. Conclusion

This work contributes a bias tees-embedded nematic liquid crystal phase shifter implemented in a meander inverted microstrip line with optimised copper-filled vias plated shut interconnecting the biasing network surface-mounted on top of a RO4003 substrate. The compact standalone solution eliminates the conventional externally-wired bias tees and junctions, meanwhile reports a 10% improvement in the figure-of-merit at 10 GHz when compared with the state-of-the-arts. The embedded device solution is momentous for deployment in the phased array feeds targeting game-changing applications such as 5G wireless communications, intelligent transportation systems, and radio astronomy.

Acknowledgment

The author would like to thank the Centre for Photonic Devices and Sensors, University of Cambridge for the training support in the NLC devices assembling. The author also thanks the supports from Imperial College London and University of Southampton.

References

[1] Robert C. Hansen, "Wiley Series in Microwave and Optical Engineering," in Phased Array Antennas , Wiley, 2010, pp.549–551.

[2] A. A. Lane, "GaAs MMIC phase shifters for phased arrays," IEE Colloquium on Solid State Components for Radar, London, UK, 1988, pp. 3/1–3/5.

[3] S. Dey, S.K. Koul, A.K. Poddar, U. Rohde, "RF MEMS switches, switching networks and phase shifters for microwave to millimeter wave applications," ISSS J Micro Smart Syst, 2020.

[4] Y. V. Kobljanskyj, G. A. Melkov, V. M. Pan, V. S. Tiberkevich and A. N. Slavin, "Active magnetostatic wave delay line for microwave signals," in IEEE Transactions on Magnetics, vol. 38, no. 5, Sept. 2002, pp. 3102–3104.

[5] A. B. Kozyrev, O. I. Soldatenkov, A. V. Ivanov, S. Y. Ivanova and L. Sengupta, "Electrically controlled ferroelectric delay line," 13th International Crimean Conference Microwave and Telecommunication Technology, Sevastopol, Crimea, Ukraine, 2003, pp. 481–482.

[6] J. Li and D. Chu, "Liquid crystal-based enclosed coplanar waveguide phase shifter for 54–66 GHz applications," Crystals, vol. 9, 12, 650, Dec. 2019.

[7] L. Cai, H. Xu, J. Li, and D. Chu, "High figure-of-merit compact phase shifters based on liquid crystal material for 1–10 GHz applications," Jpn. J. Appl. Phys., vol. 56, 011701, Nov. 2017.

[8] J. Li, "Structure and Optimisation of Liquid Crystal based Phase Shifter for Millimetre-wave Applications," Apollo, University of Cambridge Repository, doctoral thesis, Jan. 2019.

[9] D. C. Zografopoulos, A. Ferraro, and R. Beccherelli, "Liquid-crystal high-frequency microwave technology: Materials and Characterization," Adv. Mater. Technol., vol.4, 2, 1800447, Dec. 2018.

[10] J. Li, H. Xu, and D. Chu, "Design of liquid crystal based coplanar waveguide tunable phase shifter with no floating electrodes for 60–90 GHz applications," in 2016 46th European Microwave Conference (EuMC), London, 2016, pp. 1047–1050.

[11] L. Cai, H. Xu, J. Li, and D. Chu, "High FoM liquid crystal based microstrip phase shifter for phased array antennas," in 2016 International Symposium on Antennas and Propagation (ISAP), Okinawa, 2016, pp. 402–403.

[12] A. Yontem, J. Li, and D. Chu, "Imaging through a projection screen using bi-stable switchable diffusive photon sieves," Opt. Express, vol. 26, Apr. 2018, pp. 10162–10170.

[13] S. Muller, P. Scheele, C. Weil, M. Wittek, C. Hock, and R. Jakoby, "Tunable passive phase shifter for microwave applications using highly anisotropic liquid crystals," Proceedings of the IEEE MTT-S International Microwave Symposium Digest, Fort Worth, TX, USA, 6–11 June 2004, pp. 1153–1156.

[14] J. Li, "Numerical Solution of One-Speed One-Dimensional Diffusion Equation based on Finite Difference and Source Iteration," SSRN Electronic Journal, June 2020. doi: 10.2139/ssrn.3633159

[15] J. Li, “Computational Perturbation Methods for Moderator and Doppler Temperature Coefficients in the European Pressurised Reactor Core Analysis,” 3rd IEEE International Conference on Computer, Electrical & Communication Engineering (ICCECE), Southend, 2020, pp. 201–204.

[16] X. Guo and J. Li, “A Novel Twitter Sentiment Analysis Model with Baseline Correlation for Financial Market Prediction with Improved Efficiency,” 2019 Sixth International Conference on Social Networks Analysis, Management and Security (SNAMS), Granada, Spain, 2019, pp. 472–477.

[17] J. Li and X. Guo, “COVID-19 Contact-tracing Apps: A Survey on the Global Deployment and Challenges,” arXiv preprint arXiv:2005.03599, 2020.

[18] J. Li, “Fault-Event Trees Based Probabilistic Safety Analysis of a Boiling Water Nuclear Reactor’s Core Meltdown and Minor Damage Frequencies,” Safety, vol. 6, 2, 28, June 2020.

[19] J. Li, “Public Perceptions of Nuclear Energy in the Post-Fukushima World,” SSRN Electronic Journal, June 2020. doi: 10.2139/ssrn.3625941

[20] J. Li, “Multi-ring Subgroup Method in Characterising Highly Self-shielded Gadolinia Burnable Poison Pins for the UK EPR Nuclear Fuel Assembly,” 3rd IEEE International Conference on Computer, Electrical & Communication Engineering (ICCECE), Southend, 2020, pp. 196–200.

[21] J. Li, “Navigating COVID-19 and Brexit Uncertainties for the 2030 Challenge of Nuclear Renaissance in the UK,” SSRN Electronic Journal, July 2020. doi: 10.2139/ssrn.3664580

[22] J. Li, “Modelling nuclear fuel assembly with thermal-hydraulic feedback and burnup using WIMS-PANTHER-Serpent,” Journal of Physics: Conference Series, 2020.

[23] J. Li, “Design of a Four-stage Pipelined Reduced Instruction Set Computing Microprocessor,” SSRN Electronic Journal, June 2020. doi: 10.2139/ssrn.3615850

[24] J. Li, “Vulnerabilities Mapping based on OWASP-SANS: A Survey for Static Application Security Testing (SAST)”, Annals of Emerging Technologies in Computing (AETiC), vol. 4, no. 3, pp. 1–8, July 2020.

[25] J. Li and X. Guo, “Global Deployment Mappings and Challenges of Contact-tracing Apps for COVID-19,” SSRN Electronic Journal, May 2020. doi: 10.2139/ssrn.3609516

[26] J. Li, “60 GHz Optimised Nickel-free Gold-plated Enclosed Coplanar Waveguide Liquid Crystal Phase Shifter,” International Microwave Workshop Series on Advanced Materials and Processes for RF and THz Applications (IEEE MTT-S IMWS-AMP), Suzhou, 2020.

[27] J. Li, “Millimetre-wave beam steering with analog-resolution and minimised distortion based on liquid crystals tunable delay lines with enhanced signal-to-noise ratios,” Proc. SPIE, Millimetre Wave and Terahertz Sensors and Technology, SPIE Security + Defence, Edinburgh, 2020.

[28] J. Li, “Low-loss tunable dielectrics for millimeter-wave phase shifter: from material modelling to device prototyping,” IOP Conference Series: Materials Science and Engineering, vol. 892, 012057, 2020.

[29] J. Li, “All-optically Controlled Microwave Analog Phase Shifter with Insertion Losses Balancing,” Engineering Letters, vol. 28, no. 3, pp. 663–667, 2020.